

Analysis and Modeling of *PVTX* Diagram of an Unsaturated Polyester Resin, Thermoplastic Additive, and Mineral Fillers Blend

N. Boyard,¹ M. Vayer,¹ C. Sinturel,¹ R. Erre,¹ D. Delaunay²

¹Centre de Recherche sur la Matière Divisée, 1 B rue de la Férellerie, 45071 Orleans Cedex 02, France

²Ecole Polytechnique de l'Université de Nantes—Laboratoire de Thermocinétique, Rue Christian Pauc, 44306 Nantes, France

Received 30 January 2002; accepted 7 June 2002

Published online 19 February 2003 in Wiley InterScience (www.interscience.wiley.com). DOI 10.1002/app.11830

ABSTRACT: We studied the dynamic curing of a polymer blend containing an unsaturated polyester prepolymer, styrene, and a saturated polyester as a low-profile thermoplastic additive during heating from 40 to 160°C with a constant rate (4 or 10 K/min). This work was performed by means of a homemade dilatometer that simultaneously determined conversion degree, volume, pressure, and temperature. The various phenomena inducing volume change were identified and then separated (thermal expansion,

shrinkage, and shrinkage compensation). A model based on physical consideration was built that allowed an accurate fit of the experimental results. The influence of the pressure on all this phenomena was summarized and quantified. © 2003 Wiley Periodicals, Inc. *J Appl Polym Sci* 88: 1258–1267, 2003

Key words: thermosets; curing of polymer; simulations

INTRODUCTION

The cure of unsaturated polyester (UP) and styrene generates polymerization shrinkage that induces stresses in the bulk of the cured thermoset material and consequently deformations, especially at the surface.¹ The addition of a thermoplastic additive [low-profile additive (LPA)] helps to solve this problem by inducing a phase separation^{2,3} that allows release of stresses at the interfaces between cured UP and LPA.^{4,5} The formation of this two-phase structure is necessary for shrinkage compensation.^{5,6} The shrinkage control mechanism of blends containing thermoplastic, unsaturated polyester prepolymer, and styrene has been extensively studied and described.^{7–11} It is generally agreed that this shrinkage control proceeds mainly by formation of pores,^{12–14} although thermal expansion and contraction during heating and cooling, respectively, also affect shrinkage. To our knowledge, the quantification and description of the formation and release of stresses were described only by Chan-Park et al.¹² The effects of LPA concentration and type,¹⁵ UP resin structure,¹⁶ and processing conditions^{13,17,18} on shrinkage control have been well in-

vestigated, generally with a dilatometer. Traditionally, the equipment is used to investigate volume changes during thermoset polymer processing and measures only pressure, volume, and temperature. The conversion degree is generally measured by DSC,¹³ which tends to be prejudicial against a wholly accurate interpretation. Indeed, the four variables of pressure, volume, time, and conversion degree (P , V , T , and X , respectively) need to be considered simultaneously to describe the system. Moreover, these studies are frequently performed under isothermal curing conditions to avoid thermal expansion^{13,17,18} and generally at low temperature (30–85°C range) to slow down the reaction rate. However, the industrial curing behavior corresponds to dynamic curing where the cold uncured material is injected in the hot mold.

The curing kinetics of unsaturated polyester resin has been extensively studied by Salla and coworkers.^{19–22} The phenomena inducing a volume change during thermoset blend heating have been identified, that is, thermal expansion, polymerization shrinkage, and shrinkage compensation.¹³ Hill et al.¹⁸ proposed two models to predict the volume change during isothermal curing. One is based on conversion degree and the other is based on radical concentration. Although these two models include both thermal effects and polymerization shrinkage effect they do not take into account shrinkage compensation.

As a matter of fact, a model to predict volume change during dynamic curing has to be defined to include shrinkage compensation. To achieve this goal,

Correspondence to: D. Delaunay (didier.delaunay@polytech.univ-nantes.fr).

Contract grant sponsor: La Region Centre.

Contract grant sponsor: Menzolit Society.

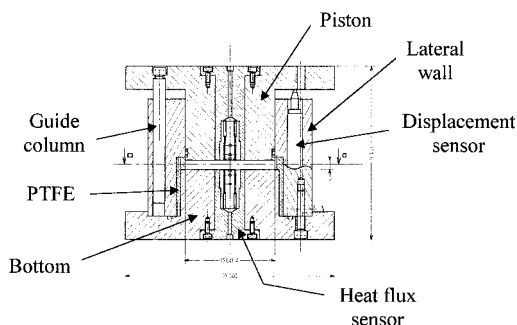


Figure 1 Cutaway view of the dilatometer configuration.²³

experiments were performed with a home-built apparatus, where volume change and conversion degree were measured simultaneously. A model for dynamic curing was developed based on these experimental results. This model took into account thermal expansion, polymerization shrinkage, and associated shrinkage compensation. The experiments were performed with a low weight saturated polyester, as LPA, rarely used and studied in the literature.

EXPERIMENTAL

Materials

The thermoset blend used in this work was based on an unsaturated polyester prepolymer (14.0 wt %), styrene (6.8 wt %) as curing agent, and a thermoplastic additive (3.7 wt %) as shrinkage compensation agent. Ter-butyl perbenzoate as polymerization initiator (0.3 wt %), calcium stearate as demolding agent (1.3 wt %), calcium carbonate as mineral filler (73.3 wt %), and parabenzoquinone (0.6 wt %) as inhibitor were also added to this blend.

The unsaturated polyester prepolymer ($M_n = 2700 \text{ g mol}^{-1}$) was made from a 1 : 0.7 : 0.3 mixture of maleic anhydride, propylene glycol, and neopentyl glycol.

The LPA ($M_n = 2690 \text{ g mol}^{-1}$) was a saturated polyester based on adipic acid and propylene glycol. The molar ratio of styrene/unsaturated polyester prepolymer was set at a value of 2.0. The LPA content based on pure saturated polyester solid was 15% of the total weight of the ternary blend unsaturated polyester/styrene/LPA.

Instrumentation and procedures

The device used for measurements is shown in Figure 1, a detailed description of which is given in Millischer et al.²³ The sample, a 60.4-mm-diameter disk was compressed between the mold bottom and a mobile piston moving inside the cylindrical lateral wall of the stainless steel mold. The piston moved following the variations of the sample volume. The piston dimensions were such that the pressure in the sample was sup-

posed to be hydrostatic. The pressure in the molding cavity (up to 7.5 MPa) was controlled within 7×10^{-2} MPa precision. The mold was placed between the heating plates of a press, equipped with a displacement sensor that measured the thickness variations of the disk. This LVDT-type sensor can measure displacements of 10 mm with a precision of $1 \mu\text{m}$. Heat flux sensors, placed in the bottom of the mold and in the piston, used thermocouples placed inside the sensor at different distances of the surface. These sensors, which do not modify the measured fluxes, were conceived at the laboratory and are described in detail in Masse et al.²⁴ The temperature data were treated by a classical inverse sequential method²⁵ and the temperature and heat flux densities to the surface of the sensor were so determined. The precision of heat fluxes was estimated to 0.5%. We can therefore reach the heat flux generated by the cure reaction. A classical technique was applied to the heat fluxes, analogous to the measurements in differential scanning calorimetry. The enthalpy and the conversion degree of the reaction can be determined. The mold was designed so that the heat transfers would be unidirectional in the direction of the axis of the disk. The temperature and conversion degree gradients in the sample under heating were limited, considering its small thickness and the small heating rate, verified by calculations.²⁶

The sample weight before curing was adjusted ($\approx 15 \text{ g}$) to mold a cylinder with a thickness of 5 mm. A scanning run of temperature was composed of two identical cycles. The cycle started at 40°C for 15 min and increased linearly to 160°C . The temperature of 160°C was maintained for 15 min then decreased to 40°C .

The data collected during the second cycle were used to calibrate heat flux and thickness. During the first cycle, the measured heat flux was ascribed to the polymerization exothermal reaction and sample heat capacity before, during, and after curing. The observed heat flux during the second cycle was attributed only to the heat capacity of the cured blend. To eliminate heat capacity variation of the blend before and after curing, the measured heat flux of the second cycle was subtracted from that of the first cycle, and a sigmoid function was used as baseline. When temperature increased, the mold expanded and induced a displacement detector response. Consequently, we used an aluminum standard (diameter, 60.4 mm; thickness, 5.07 mm) with known thermal expansion. The subtraction of this response to the displacement recorded for sample gave only the sample thickness. As a pressure was applied during the entire experiment, the cylindrical sample kept a constant diameter and, consequently, the sample volume change induced a change only in the sample thickness.

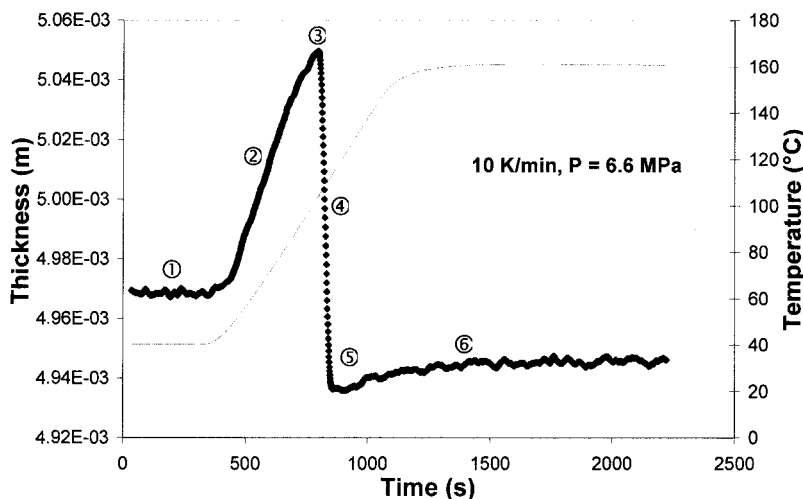


Figure 2 Evolution of the sample thickness (diamond) and temperature (full line) as a function of time for a 10 K/min heating rate and a pressure of 6.6 MPa.

Pressure in the molding cavity was either 1.3 or 6.6 MPa and the heating rate was either 4 or 10 K/min. All experimental data (heat flux and detector displacement) were analyzed and modeled with homemade programs in FORTRAN and MATLAB languages.

RESULTS

Analysis of the sample thickness

The measured thickness (e) versus time (t) for a scanning temperature (T) run of 10 K/min and a pressure (P) of 6.6 MPa is displayed in Figure 2, where six parts can be distinguished:

1. While the mold is in isothermal (40°C) conditions, e remains constant and is equal to the initial value e_0 .
2. A strong increase of e is observed at the beginning of the temperature ramp attributed to the sample thermal expansion before curing.
3. Then, the volume increases to reach a maximum. This step corresponds to a relative equilibrium between polymerization shrinkage, thermal expansion, and shrinkage compensation (if it exists at this time).
4. The thickness decreases sharply because of polymerization shrinkage.
5. The expansion of the cured sample and/or shrinkage compensation give rise to a new volume increase.
6. Finally, the temperature stabilization at 160°C leads to a constant thickness.

This curve has a classical behavior previously observed by numerous investigators.^{10,11,13,18}

Determination of the conversion degree

The relative degree of conversion X was determined by means of the exothermal heat flux generated by the reticulation reaction and is defined by the following equation:

$$X = \frac{\int_0^t \Phi dt}{\Delta H_{\text{total}}} \quad (1)$$

where Φ is the measured heat flux and ΔH_{total} is the polymerization reaction heat given by

$$\Delta H_{\text{total}} = \int_0^{t_f} \Phi dt$$

where t_f is the time at the end of the reaction.

Figure 3 shows the exothermal flux and the relative conversion degree X as a function of time t for the experimental conditions of Figure 2. This figure has a classical behavior. Experiments did not show any dependency on pressure but the heating rate evidently exerts an influence because of the kinetic effect (see, e.g., Salla et al.²²).

Modeling the thickness changes

As mentioned before, during the thermal cycle, different phenomena such as thermal expansion and contraction, polymerization shrinkage, and shrinkage compensation (i.e., pore formation) exist, or can exist. These various contributions must be separated to

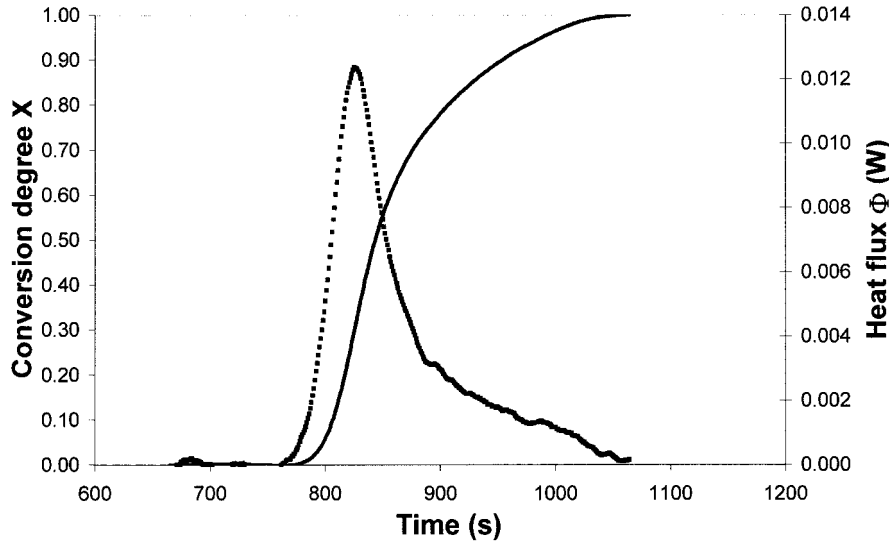


Figure 3 Heat flux Φ (square) and conversion degree X (full line) of the copolymerization reaction as a function of time for a 10 K/min heating rate and a pressure of 6.6 MPa.

model the behavior of the thermoset material during nonisothermal curing.

The state equation describing the variation of the specific volume (v) of the blend is

$$\frac{dv}{v} = \frac{1}{v} \left(\frac{\partial v}{\partial T} \right)_{P,X} dT + \frac{1}{v} \left(\frac{\partial v}{\partial X} \right)_{P,T} \times dX + \frac{1}{v} \left(\frac{\partial v}{\partial P} \right)_{T,X} dP \quad (2)$$

Because the pressure P in the mold cavity is constant, eq. (2) can be simplified to

$$\frac{dv}{v} = \alpha_v dT + R_v dX \quad (3)$$

where $\alpha_v = (1/v)(\partial v/\partial T)_{P,X}$ is the volumetric thermal expansion and $R_v = (1/v)(\partial v/\partial X)_{P,T}$ is a volumetric coefficient associated with polymerization.

Given that the sample is a cylinder with constant diameter, eq. (3) is equivalent to

$$\frac{de}{e} = \alpha dT + R dX \quad (4)$$

where $\alpha = (1/e)(\partial e/\partial T)_{P,X}$ is the linear thermal expansion coefficient, a function of T , P , and X ; and $R = (1/e)(\partial e/\partial X)_{P,T}$ is the linear coefficient characterizing the shrinkage and shrinkage compensation and is a function of T , P , and X .

Equation (4) can be rewritten:

$$de = \alpha(X, T, P)e dT + R(X, T, P)e dX \quad (5)$$

Because the measured parameter is e , integration of eq. (5) gives

$$\int_0^t de = \int_{T_0}^{T_0+\Delta T} e(t)\alpha(X, T, P) dT + \int_0^X e(t)R(X, T, P) dX \quad (6)$$

which can be also rewritten as

$$e(t) = e_0 + \int_{T_0}^{T_0+\Delta T} e(t)\alpha(X, T, P) dT + \int_0^X e(t)R(X, T, P) dX \quad (7)$$

The thickness at time t is the sum of the initial thickness e_0 , the thickness variation attributed to the temperature variation (Δe_T) [i.e., thermal expansion or contraction (second term of the right-hand side)], and the contribution of cure phenomena (shrinkage and the associated compensation) to the thickness variation of the sample (Δe_{SC}) (third term of the right-hand side).

Modeling the thermal expansion

To be able to consider only thickness changes attributed to phenomena associated with reticulation, we

TABLE I
Experimental Thermal Expansion Coefficients of Samples Before and After Curing
for the Different Processing Conditions

Experimental condition	10 K/min, 1.3 MPa	10 K/min, 6.6 MPa	4 K/min, 1.3 MPa	4 K/min, 6.6 MPa
α before curing (10^{-4} K^{-1})	3.9	2.9	4.3	3.3
α after curing (10^{-4} K^{-1})	0.3	0.3	0.2	0.3

estimated Δe_T . For this purpose, estimation of $\alpha(X, T, P)$ was needed.

Before curing, thermal expansion corresponded to the uncured sample (part ② of the curve in Fig. 2). $e(t)$ was a quasi-linear function of the temperature, meaning that $\alpha(0, T, P)$ was a constant value, independent of the temperature. Consequently, the expansion coefficient of the sample before curing could be easily determined by the slope of the $e = f(T)$ curve.

After curing, additional heating did not modify the polymerization. The sample thickness in the second cycle was also a linear function of the temperature. The thermal expansion coefficient $\alpha(1, T, P)$ was also constant, independent of the temperature.

During copolymerization, the blend proceeded from a fluid state to a rubbery state. The blend was then considered as an ideal mixture for $0 < X < 1$, with the coexistence of both uncured and cured phases. As a consequence, the thermal expansion coefficient was given by

$$\alpha(X, T, P) = (1 - X)\alpha(0, T, P) + X\alpha(1, T, P) \quad (8)$$

The thermal expansion coefficients are listed in Table I. The coefficients were determined within $3 \times 10^{-5} \text{ K}^{-1}$ precision. As a consequence, we considered that obtained values did not depend on the heating rate. The thermal expansion coefficient before curing de-

pended on pressure but after curing they were insensitive to pressure.

Figures 4 and 5 represent $(e(t) - \Delta e_T)$ (i.e., thickness evolution versus time only attributed to polymerization phenomena for 1.3 and 6.6 MPa, respectively). The shapes of the curves were in agreement with those expected. First of all, thickness was constant and equal to e_0 until the start of copolymerization. Then, sample thickness decreased drastically with resin shrinkage. Finally, thickness decrease stopped. If shrinkage remained, it was compensated by formation of pores. For longer times, the reticulation was complete and the thickness remained constant, given that cured resin thermal expansion was the only observed phenomenon.

Kinetics of thickness evolution relative to polymerization phenomena

To identify precisely the various coupled phenomena governing the thickness evolution, we plotted $(d/dt)[e(t) - \Delta e_T]$, which represents the thickness evolution rate V_{SC} , as a function of the conversion rate dX/dt .

Theoretically, this rate has two components: the thickness evolution rate V_S (S for shrinkage), attributed to polymerization shrinkage, and the thickness

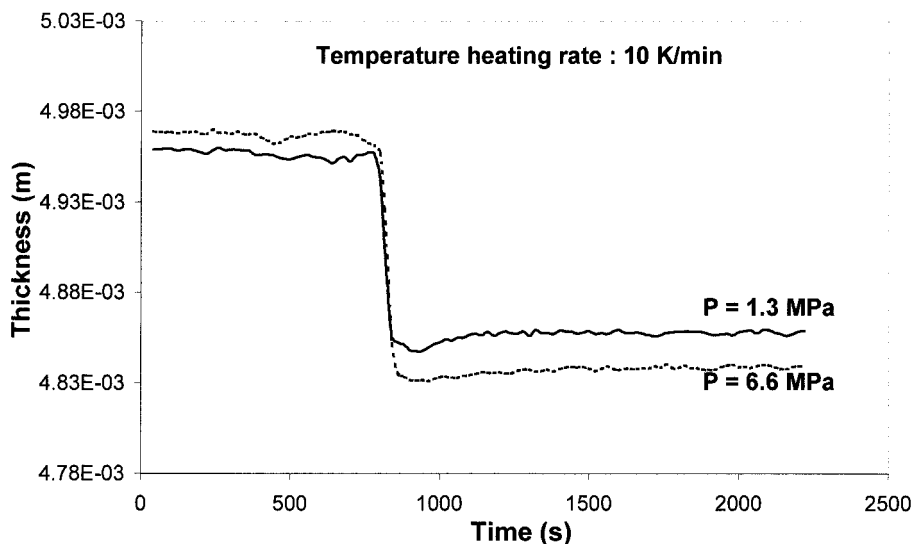


Figure 4 Thickness versus time without thermal expansion contribution $e(t) - \Delta e_T = f(t)$ for a heating rate of 10 K/min and a pressure of 1.3 MPa (full line) and 6.6 MPa (dashed line).

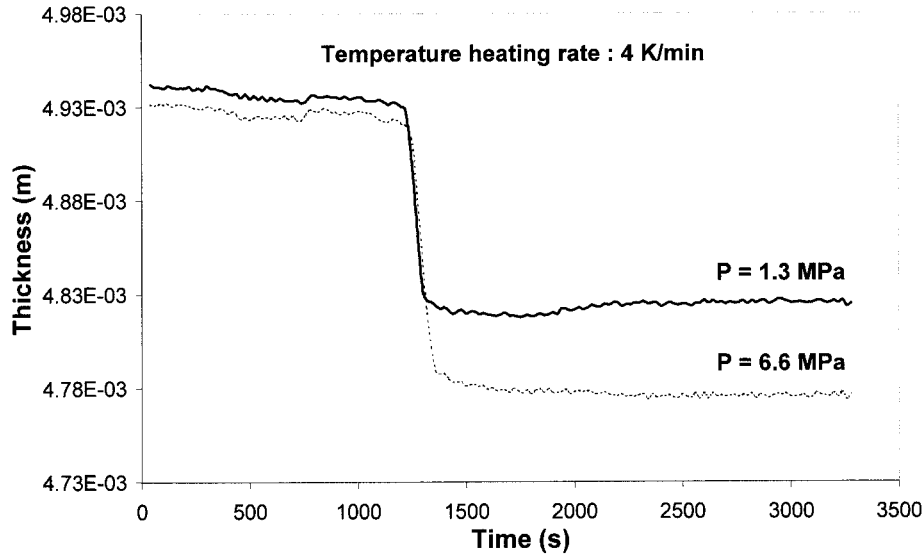


Figure 5 Thickness versus time without thermal expansion contribution $e(t) - \Delta e_T = f(t)$ for a heating rate of 4 K/min and a pressure of 1.3 MPa (full line) and 6.6 MPa (dotted line).

evolution rate V_C (C for shrinkage compensation), attributed to the shrinkage compensation, if it exists.

Figure 6 presents V_{SC} versus dX/dt for 10 K/min and 1.3 MPa pressure. This curve can be separated into four parts:

1. V_{SC} remains zero up to $X = X_1$. We suppose that up to X_1 , no macroscopic manifestation of shrinkage is visible.
2. V_{SC} is a linear function of dX/dt . This simple relation observed in our case up to X_{Ci} was postulated by Hill¹⁸ during the entire time of copolymerization. Supposing that shrinkage was the only phenomenon existing at this moment, we assumed the strong hypothesis that this relation is valid whatever the X value. Consequently, this part of the

curve allows us to define V_S as a linear function of dX/dt . Complementary experiments will be carried out to validate this hypothesis more rigorously.

3. From $X = X_{Ci}$ up to $X = X_{Cf}$, a sharp decrease of the absolute value of V_{SC} is observed, clearly indicating that another phenomenon is superposed to shrinkage. We call this period between X_{Ci} and X_{Cf} where the shrinkage compensation is setting up, the transition period.
4. Finally, V_{SC} versus dX/dt is a linear function whose slope is very small, resulting from the superposition of shrinkage and the associated compensation.

From these results, we can isolate the shrinkage compensation. The evolution of V_C versus dX/dt can

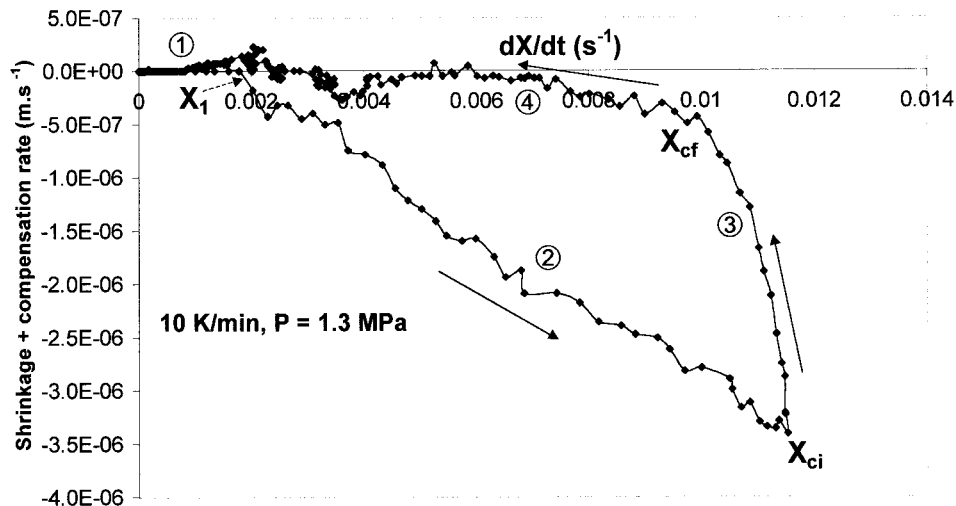


Figure 6 Thickness evolution rate V_{SC} as a function of conversion rate dX/dt for a heating rate of 10 K/min and pressure of 1.3 MPa. Arrows indicate the direction of the displacement on the curve. The starting point is (0,0).

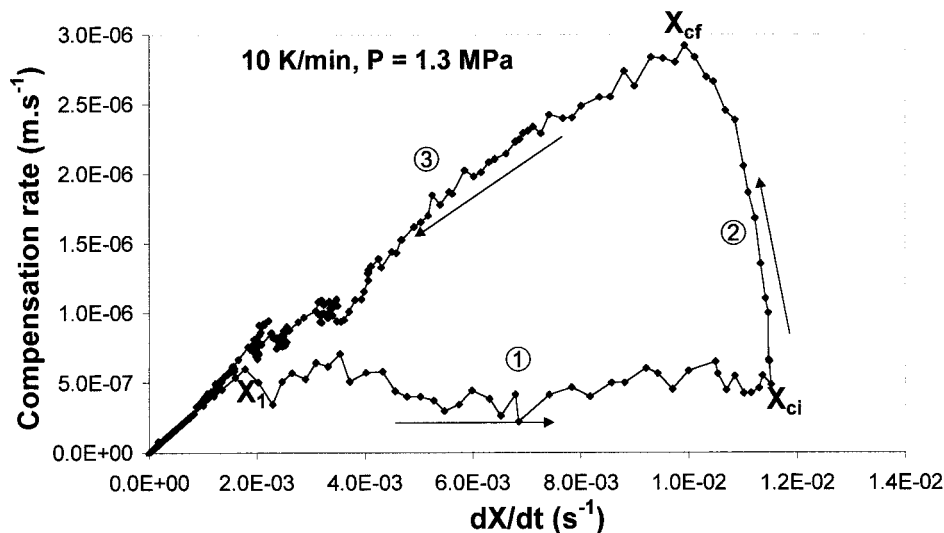


Figure 7 V_C as a function of the conversion rate dX/dt for a heating rate of 10 K/min and pressure of 1.3 MPa. Arrows indicate the direction of the displacement on the curve. The starting point is (0,0).

be indeed determined by subtracting V_S from V_{SC} . The obtained curve is presented in Figure 7, where three periods can be distinguished:

1. Up to $X < X_{Ci}$, V_C remains equal to 0, in theory. The low observed value is a consequence of experimental noises and errors on graphical V_S determination.
2. In the transition zone, between X_{Ci} and X_{Cf} , the shrinkage compensation mechanism is setting up. V_C increases rapidly to a maximum value; this increase is not linear.
3. Then V_C decreases linearly to zero.

Considering the previous results, we propose the following model to describe the rate of thickness evolution attributed to polymerization. V_{SC} can be expressed as the sum of shrinkage rate and shrinkage compensation rate:

First step. When $X < X_1$, $V_{SC} = 0$.

Second step. When $X_1 < X < X_{Ci}$, $V_{SC} = V_S$, where $V_S = K_S e_0 (dX/dt)$.

K_S is a coefficient related to the volume contraction attributed to the opening of double bonds. This shrinkage coefficient K_S is not dependent on the heating rate in a first approximation but can be sensitive to the pressure.

Third step. When $X_{Ci} < X < X_{Cf}$ (transition period), $V_{SC} = V_S + V_C$, where $V_S = K_S e_0 (dX/dt)$ and $V_C = K_C e_0 (dX/dt)$.

Because K_C corresponds to the volume expansion associated with stress release, it must be sensitive to the pressure and be insensitive to the heating rate in a first approximation. The compensation coefficient K_C evolves with time and we propose to represent it by

the following expression: $K_C = K_{Cmax}[1 - F(X)]$, where $F(X) = \exp[-(AX^4 + B)^2]$.

This F function has specific properties. It is equal to 1 for $X < X_{Ci}$. It becomes progressively equal to 0 between X_{Ci} and X_{Cf} . Its derivatives at X_{Ci} and X_{Cf} are equal to zero. Consequently, A and B are functions of X_{Ci} and X_{Cf} and are given by $A = 2.5/(X_{Cf}^4 - X_{Ci}^4)$ and $B = 2.5 - AX_{Cf}^4$. The constant value 2.5 is adjusted to fit the experimental results. The evolution of K_C versus X is shown in Figure 8.

Fourth step. When $X_{Cf} < X$, $V_{SC} = V_S + V_C$, where $V_S = K_S e_0 (dX/dt)$ and $V_C = K_{Cmax} e_0 (dX/dt)$.

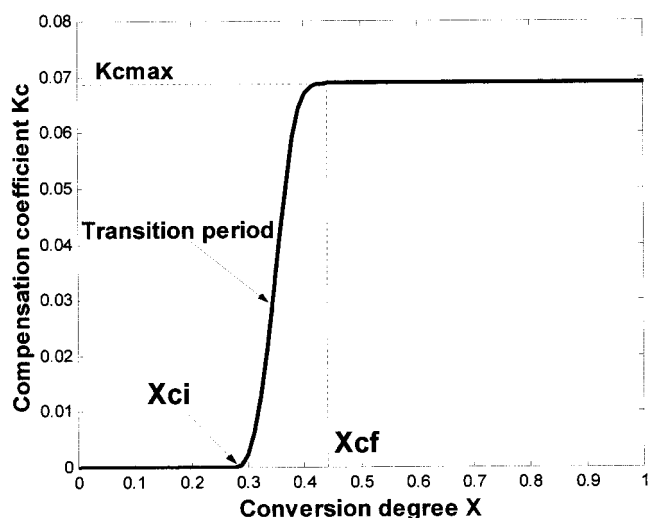


Figure 8 Compensation coefficient K_C versus conversion degree during the transition period for a heating rate of 10 K/min and a pressure of 1.3 MPa.

TABLE II
Fitted Parameters for the Different Experimental Conditions, Values of σ , and Amplitudes of Various Identified Phenomena

Experimental conditions	4 K/min 1.3 MPa	10 K/min 1.3 MPa	4 K/min 6.6 MPa	10 K/min 6.6 MPa
Fixed parameters				
X_1 (%)	1.0	4.5	5.0	3.9
X_{Ci}	30	28	42	39
Fitted parameters				
K_S (10^{-2})		-6.9		-6.1
K_{Cmax} (10^{-2})		6.8		5.8
X_{Cf}	42	42	63	57
σ (m)	4×10^{-6}	4×10^{-6}	4×10^{-6}	3×10^{-6}
Total thermal expansion (%) $\Delta e_T/e_0$	3.0	3.0	2.4	2.3
Total variation due to shrinkage (%) $\Delta e_S/e_0$	-6.8	-6.6	-5.8	-5.9
Total variation due to shrinkage compensation (%) $\Delta e_C/e_0$	7.5	7.3	5.3	5.4
Total variation (%) $(\Delta e_C + \Delta e_S + \Delta e_T)/e_0$	0.6	0.9	-0.6	-0.7
Transition period length X_{Cf} (%)	12	14	21	18
Δe_C (transition zone)/ Δe_C tot (%)	10	13	23	17

Reconstruction of the sample thickness evolution

The evolution of the sample thickness during the thermal cycle is represented by a sum of contributions associated with thermal expansion Δe_T and with polymerization phenomena Δe_{SC} . This latter is a sum of contributions from both polymerization shrinkage and shrinkage compensation.

$$e(t) = e_0 + \Delta e_{SC} + \Delta e_T = e_0 + \Delta e_S + \Delta e_C + \Delta e_T \quad (9)$$

The contribution from thermal expansion Δe_T is obtained by

$$\Delta e_T = \int_{T_0}^{T_0+\Delta T} (e_0 + \Delta e_{SC}) \alpha(X, T, P) dT$$

where ΔT is the temperature variation between T_0 and T .

The contribution from polymerization phenomena Δe_{SC} may be expressed as

$$\Delta e_{SC} = \int_{t_0}^{t_0+\Delta t} V_{SC} dt \quad (10)$$

where Δt is the temperature variation between t_0 and t .

The thickness evolution Δe_{SC} during cure is separated in several steps according to the previous model: *First step.* When $X < X_1$, $V_{SC} = 0$ and $\Delta e_{SC} = 0$. Reticulation started and shrinkage effect cannot be detected.

Second step. When $X_1 < X < X_{Ci}$, shrinkage is the only observed phenomenon. $\Delta e_S = K_S e_0 (X - X_1)$, $\Delta e_C = 0$, and $\Delta e_{SC} = \Delta e_S$.

Third step. When $X_{Ci} < X < X_{Cf}$, shrinkage compensation starts but is not immediately established (transition regime). $\Delta e_S = K_S (X - X_1)$ and $\Delta e_C = \int_{X_{Ci}}^{X_{Cf}} e_0 K_C dX$.

Fourth step. When $X > X_{Cf}$, shrinkage compensation is completely established. $\Delta e_S = K_S e_0 (X - X_1)$, $\Delta e_C = (\int_{X_{Ci}}^{X_{Cf}} e_0 K_C dX) + K_{Cmax} e_0 (X - X_{Cf})$.

If the parameters of this model, X_1 , X_{Ci} , X_{Cf} , K_S , and K_{Cmax} , are known, it is possible to compute $e(t)$. To obtain values of these parameters we analyzed the experimental results with an inverse method of estimation, which is based on the minimization of the criterion $J(K_S, K_{Cmax}, X_{Cf})$ by a program using a simplex method.

$$J = \sum_{1}^N \sum_{1}^{n_i} (e_0 + \Delta e_{SC} - (e - \Delta e_T))^2 \quad (11)$$

where $e_0 + \Delta e_{SC}$ is the thickness calculated for each experimental value (time step), $e - \Delta e_T$ is the experimental thickness corrected of thermal expansion effect, N is the number of experiments, and n_i is the number of experimental values for experiment i .

Note that we use two experiments (for two different heating rates) corresponding to the same pressure to compute the criterion J . Indeed, we assume here that K_S and K_C are independent of the heating rate. For the inverse calculation, X_1 and X_{Ci} are fixed and obtained from experimental considerations (see example in Fig. 6) for each experiment. For a given pressure, we identify a set of values K_S , K_{Cmax} and X_{Cf1} and X_{Cf2} (the subscripts 1 and 2 are relative to the two experiments used to compute J).

The theory of inverse method²⁵ shows that the fitted parameters correspond to an acceptable solution if σ_i

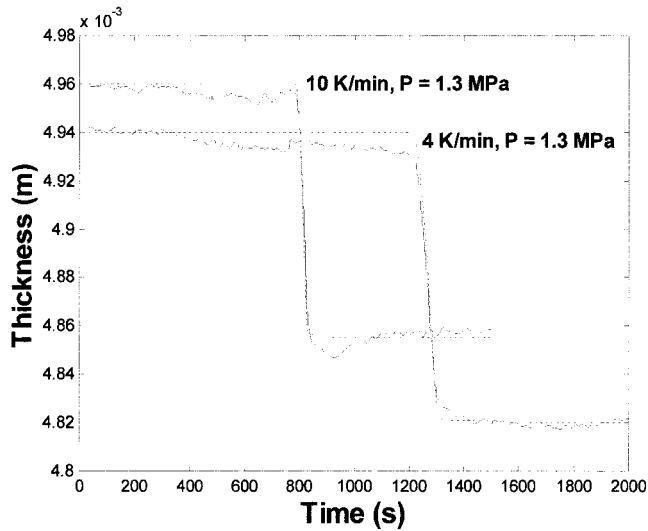


Figure 9 Comparison between experimental (full line) and modeled (dashed line) curves representing thickness versus time without taking into account thermal expansion for a pressure of 1.3 MPa.

$= (J_i/n_i)^{1/2}$ is equal to or lower than the error of the experimental value ($5 \mu\text{m}$).

The K_S , $K_{C_{\text{max}}}$, X_{Cf1} , and X_{Cf2} optimized values are reported in Table II. The thickness evolution curves thus modeled were compared to the experimental curves both without and with taking into account the thermal expansion (see Figs. 9–12). As clearly seen in these figures, the agreement is excellent. For all the experimental conditions, we verify that σ is lower than $5 \mu\text{m}$. This proves that for our experimental results, the model is adequate and the set of parameters gives an acceptable solution.

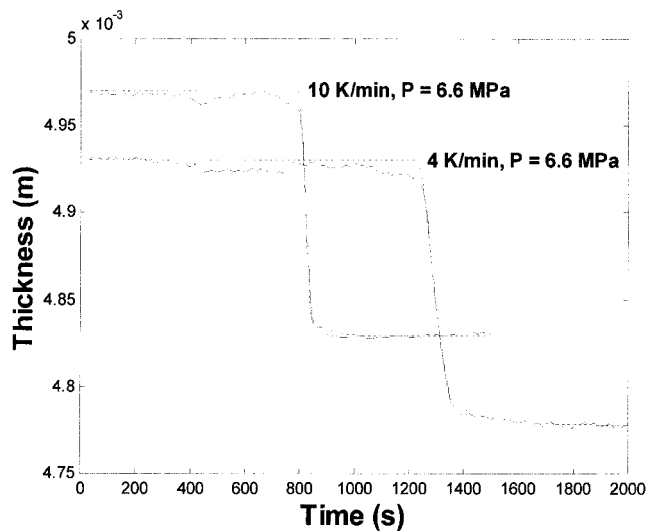


Figure 10 Comparison between experimental (full line) and modeled (dashed line) curves representing thickness versus time without taking into account thermal expansion for a pressure of 6.6 MPa.

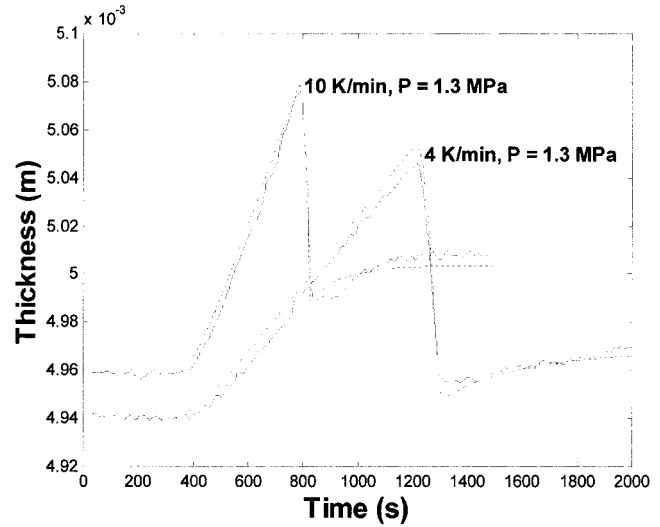


Figure 11 Comparison between experimental (full line) and modeled (dashed line) curves representing thickness versus time with taking into account thermal expansion for a pressure of 1.3 MPa.

DISCUSSION

The existence of an angular point on the $e = f(t)$ curve has already been observed and has often been presented to prove the existence of shrinkage compensation. In contrast, our results offer evidence that the shrinkage compensation phenomenon exists even if no angular point was observed and even if the final thickness revealed a shrinkage. The existence of shrinkage compensation was also verified by the presence of pores in the sample after curing. The shrinkage compensation amplitude and the measured pore volume of the cured sample were in

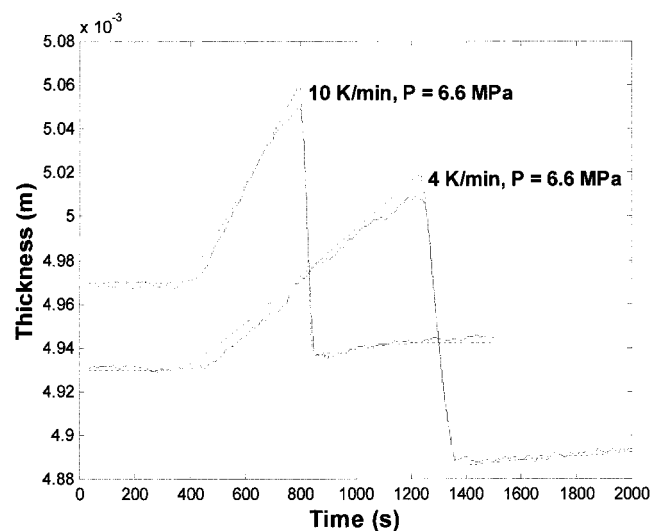


Figure 12 Comparison between experimental (full line) and modeled (dashed line) curves representing thickness versus time with taking into account thermal expansion for a pressure of 6.6 MPa.

good agreement. Our model included the polymerization shrinkage compensation, contrary to other previous models.¹⁸ It may be used to predict the polymerization shrinkage amplitude and shrinkage compensation amplitude, and to determine parameters influencing these phenomena.

Let us now consider the thickness variation of all the phenomena observed during sample heating and cure processing (Figs. 11 and 12 and Table II). K_S depends on pressure. The lower value observed for 6.6 MPa experiments can be tentatively attributed to compressibility of the material. The cumulative thermal expansion from 40°C for an uncured sample to 160°C for a cured sample is influenced by pressure and represents about half the shrinkage thickness variation. Polymerization shrinkage and shrinkage compensation are both influenced by pressure. Pressure delays compensation initially and induces a larger conversion degree transition range. Pressure induces a K_{Cmax} decrease, which was expected, considering that the applied pressure is opposed to shrinkage compensation.^{9,28} Because shrinkage induces stresses relaxed by pore formation, shrinkage and compensation are linked together.

The resulting thickness variation between an uncured sample at 40°C and a cured sample at 160°C is strongly influenced by the pressure. Indeed, a final shrinkage was observed for experiments performed at 6.6 MPa and a final expansion for experiments performed at 1.3 MPa. As noted in some previous studies,^{8,13} polymerization shrinkage is compensated by pore formation but also by thermal expansion. Pressure has a negative effect on shrinkage compensation and thermal expansion and consequently on the final shrinkage.

CONCLUSIONS

In this study, experimental results allowed us to link directly specific volume evolution and curing. A model was built to understand more deeply the implied phenomena during dynamic heating of a thermoset blend. Thermal expansion, polymerization shrinkage, and compensation were identified and separated. The cure of a sample proceeds by three steps: (1) shrinkage without compensation; (2) shrinkage and compensation setting up; and (3) shrinkage and established compensation. Polymerization and compensation shrinkage were modeled and the comparison between experiments and calculated curves exhibited excellent correlation. The model is based on two

main hypotheses: the shrinkage coefficient K_S is supposed to be constant whatever the value of X . This coefficient and the compensation coefficient K_C are independent of the thermal history $T(t)$ and depend on the pressure. Although this simple model allowed us to fit our experimental results, it could be improved by further experiments to take into account other non-detected phenomena.

This work was supported by La Region Centre and the Menzolit Society. The authors acknowledge N. Lefèvre and A. Millischer for the mold design and their assistance during dilatometer experiments.

References

- Serré, Ch.; Vayer, M.; Erre, R.; Boyard, N.; Ollive, C. *J Mater Sci* 2001, 36, 113.
- Inoue, T. *Prog Polym Sci* 1995, 20, 119.
- Hsieh, Y. N.; Yu, T. L. *J Appl Polym Sci* 1999, 73, 2416.
- Bucknall, C. B.; Partridge, I. K.; Phillips, M. J. *Polymer* 1991, 32, 636.
- Bartkus, E. J.; Kroekel, C. H. *J Appl Polym Sci* 1970, 15, 113.
- Suspene, L.; Fourquier, D.; Yang, Y. S. *Polymer* 1991, 32, 1595.
- Pattison, V. A.; Hindersinn, R. R.; Schwartz, W. T. *J Appl Polym Sci* 1974, 18, 2763.
- Atkins, K. E.; Koleske, J. V.; Smith, P. L.; Walter, E. R.; Matthews, V. E. In *Proceedings of the 31st Annual Technical Conference of the Society of Plastics Industry*, 1976.
- Ruffier, M.; Merle, G.; Pascault, J. P. *Polym Eng Sci* 1994, 33, 466.
- Kinkelaar, M.; Wang, B.; Lee, L. J. *Polymer* 1994, 35, 3011.
- Kinkelaar, M.; Lee, L. J. *J Appl Polym Sci* 1992, 45, 37.
- Chan-Park, M. B.; McGarry, F. J. *J Adv Mater* 1995, 27, 47.
- Li, W.; Lee, L. J. *Polymer* 1998, 39, 5677.
- Li, W.; Lee, L. J. *Polymer* 2000, 41, 685.
- Huang, Y. J.; Su, C. C. *Polymer* 1998, 39, 401.
- Yang, Y. S.; Lee, L. J. *Polymer* 1988, 29, 1793.
- Kinkelaar, M.; Muzumdar, S.; Lee, L. J. *Polym Eng Sci* 1995, 35, 823.
- Hill, R. R.; Muzumdar, S.; Lee, L. J. *Polym Eng Sci* 1995, 35, 852.
- Ramis, X.; Salla, J. M. *J Appl Polym Sci* 1992, 45, 227.
- Ramis, X.; Salla, J. M. *J Polym Sci Part B: Polym Phys* 1999, 37, 751.
- Ramis, X.; Salla, J. M. *J Polym Sci Part B: Polym Phys* 1997, 35, 371.
- Salla, J. M.; Cadenato, A.; Ramis, X.; Morancho, J. M. *J Therm Anal* 1999, 56, 771.
- Millischer, A.; Delaunay, D.; Jarny, Y. In *Proceedings of Cancom 2001*, Montreal, Canada, 2001.
- Masse, H.; Arquis, E.; Delaunay, D.; Quilliet, S.; Le Bot, Ph. *Int J Heat Mass Transfer*, to appear.
- Beck, J. V.; Blackwell, B.; St. Clair, C. *Inverse Heat Conduction*; Wiley-Interscience: New York, 1985.
- Millischer, A. Ph.D. Thesis, Université de Nantes, 2000.
- Vayer, M.; Serré, C.; Boyard, N.; Sinturel, C.; Erre, R. *J Mater Sci*, to appear.
- Zhang, Z.; Zhu, S. *Polymer* 2000, 41, 3861.